



# IL-27 promotes cardiac fibroblast activation and aggravates cardiac remodeling post myocardial infarction

Xiaoxue Ma<sup>a,b,1</sup>, Qingshu Meng<sup>b,c,1</sup>, Shiyu Gong<sup>d,1</sup>, Shanshan Shi<sup>b,c</sup>, Xiaoting Liang<sup>b</sup>, Fang Lin<sup>b,c</sup>, Li Gong<sup>a,b</sup>, Xuan Liu<sup>b,e</sup>, Yinzhen Li<sup>b</sup>, Mimi Li<sup>b,c</sup>, Lu Wei<sup>b,c</sup>, Wei Han<sup>f</sup>, Leng Gao<sup>g</sup>, Zhongmin Liu<sup>c,e,h,\*\*</sup>, Xiaohui Zhou<sup>b,c,\*</sup>

<sup>a</sup> Shanghai East Hospital, Jinzhou Medical University, Jinzhou, 121000, China

<sup>b</sup> Research Center for Translational Medicine, Shanghai East Hospital, Tongji University School of Medicine, Shanghai, 200120, China

<sup>c</sup> Shanghai Heart Failure Research Center, Shanghai, 200120, China

<sup>d</sup> Department of Cardiology, Shanghai East Hospital, Tongji University School of Medicine, Shanghai, 200120, China

<sup>e</sup> Department of Cardiovascular Surgery, Shanghai East Hospital, Tongji University School of Medicine, Shanghai, 200120, China

<sup>f</sup> Department of Heart Failure, Shanghai East Hospital, Tongji University School of Medicine, Shanghai, 200120, China

<sup>g</sup> Translational Medical Center for Stem Cell Therapy & Institute for Regenerative Medicine, Shanghai East Hospital, Tongji University School of Medicine, Shanghai 200123, PR China

<sup>h</sup> Shanghai Institute of Stem Cell Research and Clinical Translation, Shanghai 200120, China

## ARTICLE INFO

### Keywords:

IL-27  
Fibroblast  
Myocardial infarction  
Inflammation  
Ventricular remodeling

## ABSTRACT

Excessive and chronic inflammation post myocardial infarction (MI) causes cardiac fibrosis and progressive ventricular remodeling, which leads to heart failure. We previously found high levels of IL-27 in the heart and serum until day 14 in murine cardiac ischemia–reperfusion injury models. However, whether IL-27 is involved in chronic inflammation-mediated ventricular remodeling remains unclear. In the present study, we found that MI triggered high IL-27 expression in murine cardiac macrophages. The increased expression of IL-27 in serum is correlated with cardiac dysfunction and aggravated fibrosis after MI. Furthermore, the addition of IL-27 significantly activated the JAK/STAT signaling pathway in cardiac fibroblasts (CFs). Meanwhile, IL-27 treatment promoted the proliferation, migration and extracellular matrix (ECM) production of CFs induced by angiotensin II (Ang II). Collectively, high levels of IL-27 mainly produced by cardiac macrophages post MI contribute to the activation of CFs and aggravate cardiac fibrosis.

## 1. Introduction

Myocardial infarction (MI) remains the leading cause of morbidity and mortality worldwide [1]. Following MI, the left ventricle (LV) undergoes a series of injury and wound healing responses, including inflammation and scar formation, which are collectively

\* Corresponding author. Research Center for Translational Medicine, Shanghai East Hospital, Tongji University School of Medicine 150 Jimo Rd, Pudong, Shanghai, 200120, ORCID, China.

\*\* Corresponding author. Research Center for Translational Medicine, Department of Cardiovascular Surgery, Shanghai East Hospital, Tongji University School of Medicine 150 Jimo Rd, Pudong, Shanghai, 200120, China.

E-mail addresses: [liu.zhongmin@tongji.edu.cn](mailto:liu.zhongmin@tongji.edu.cn) (Z. Liu), [zxh100@tongji.edu.cn](mailto:zxh100@tongji.edu.cn) (X. Zhou).

<sup>1</sup> These authors contributed equally to this work.

<https://doi.org/10.1016/j.heliyon.2023.e17099>

Received 8 November 2022; Received in revised form 1 June 2023; Accepted 7 June 2023

Available online 18 June 2023

2405-8440/© 2023 The Authors. Published by Elsevier Ltd. This is an open access article under the CC BY-NC-ND license (<http://creativecommons.org/licenses/by-nc-nd/4.0/>).

referred to as LV remodeling [2,3]. Postinfarction healing and optimal scar formation play crucial roles in strengthening infarcted tissue and preventing cardiac rupture [4]. However, excessive and prolonged LV remodeling after MI leads to heart failure (HF), with a 5-year mortality of nearly 50% [5]. More intensive study is necessary to understand the mechanisms of cardiac remodeling post MI.

Multiple pathological changes occur after MI, including apoptosis of myocardial cells, activation of immune responses and fibroblasts, scar formation, and finally remodeling [6,7]. Excessive prolonged inflammatory responses contribute to persistent tissue damage and adverse ventricular remodeling post MI [8,9]. Increasing evidence suggests that inflammatory cells and cardiac fibroblasts (CFs) play central roles in cardiac fibrotic responses during pathological cardiac remodeling [10,11]. In the chronic inflammatory period post MI, macrophages contribute to adverse cardiac remodeling by secreting cytokines that promote CFs activation [12,13]. Upon activation, CFs differentiate into myofibroblasts, express  $\alpha$ -smooth muscle actin ( $\alpha$ -SMA), and act as the main source of extracellular matrix (ECM) proteins [14,15]. Excessive collagen deposition leads to cardiac fibrosis and ventricular remodeling.

Interleukin-27 (IL-27), including an alpha subunit IL-27p28 and a beta subunit Epstein–Barr virus-induced protein 3 (EBI3), is a member of the interleukin-12 (IL-12) family [16,17]. IL-27 is mainly produced by activated antigen-presenting cells (APCs), such as monocytes, macrophages, and dendritic cells (DCs) [18]. Previous clinical evidence demonstrated that serum IL-27 levels in acute MI and unstable angina patients were significantly upregulated compared to those in controls [19]. Our previous study revealed high levels of IL-27 in both injured heart and serum and the elevation maintained until a chronic phase post myocardial infarction/reperfusion (MI/R) [20]. Moreover, addition of IL-27 increased the production of type I collagen in cultured human fibroblasts from the patients with systemic sclerosis [21]. However, the role of IL-27 in cardiac fibroblasts, a key cell type involved in ventricular remodeling, has not been elucidated. In the present study, we explored whether IL-27 regulates the function of cardiac fibroblasts and contributes to cardiac remodeling, as well as the relevant signaling pathways.

## 2. Materials and methods

### 2.1. Mice

Eight-week-old male C57BL/6 mice (Beijing Vital River Laboratory Animal Technology Co., Ltd.) that weighed 20–22 g were raised under specific pathogen-free (SPF) conditions in an environment with constant temperature (23–24 °C), humidity (55 ± 5%), and light (12:12 of day: night). Neonatal C57BL/6 mice (1–3 days old) were used for cell isolation. All animal procedures were performed in accordance with the Institutional Animal Care and Use of Laboratory Animals approved by Tongji University (TJBB00121101).

### 2.2. Establishment of the murine MI model

Murine MI models were established as previously described [22]. The mice were randomly divided into a sham operation group and an MI group. Briefly, mice were anesthetized with sodium pentobarbital (50 mg/kg) intraperitoneally. They were intubated and put on the ventilator. MI was induced by permanent ligation of the left anterior descending (LAD) artery with 8-0 sutures. Successful myocardial ischemia is marked by paleness of the anterior wall of the left ventricle. Mice with exposed hearts through left thoracic incision without LAD were used as the sham operation group. Mice were closely observed after the operation for their full recovery. Experiments were carried out at different time points after surgery, and there were at least 8 mice in the sham or MI groups.

### 2.3. Echocardiography

Echocardiography was used to assess cardiac systolic and diastolic function as previously described [23]. A Visual Sonics high-resolution Vevo2100 ultrasound system (VisualSonics, Canada) with a 30-MHz linear array ultrasound transducer (VisualSonics, Canada) was applied. In brief, mice were anesthetized with 1.0% isoflurane until the heart rate stabilized. Parasternal long-axis images were acquired in B-mode with the scan head in an appropriate position to identify the maximum LV length. In this view, the M-mode cursor was positioned perpendicular to the maximum LV dimension in end-diastole and systole, and M-mode images were obtained for measuring wall thickness and chamber dimensions. LV ejection fraction (EF) and LV fractional shortening (FS) were calculated automatically.

### 2.4. Tissue collection and preparation

Samples were collected at different time points after the surgery. Mice were anesthetized with 1% sodium pentobarbital. Whole blood was collected by removing the eyes, left at room temperature for 30 min, and then centrifuged at 1000×g for 10 min, and the serum was collected and stored at –80 °C for ELISA. Mice were sacrificed on days 0, 1, 3, 7, 14 and 28 after surgery, and then hearts were perfused with precooled 1X PBS and collected for ELISA or histological analysis. Apical heart samples below the ligature line weighing approximately 50–100 mg were used for ELISA. Five times the mass volume of 1X PBS containing 1% PMSF (#36978, Thermo Fisher, USA) was added to the samples. Tissues were cut as small as possible by using scissors and then sonicated (Thermo Fisher, USA) at a power of 25% for 2 s with 5 s intervals for a total time of 2 min. The samples were sonicated at 4 °C for 3 min. After sonication, samples were lysed at 4 °C for 30 min. Then, these samples were centrifuged at 12000×g for 10 min, and the supernatants were collected and stored at –80 °C. The protein concentrations were quantified using a bicinchoninic acid (BCA) protein assay kit (Thermo Fisher, USA).

## 2.5. ELISA for quantification of IL-27

The IL-27 levels in serum and heart tissue were detected by the Mouse IL-27 ELISA Kit (Multiscience, China) according to the manufacturer's protocol. Standards of IL-27 and all samples were analyzed in triplicate. Standard curves were created using the CurveExpert 1.3 software program (Hymas developers).

## 2.6. Masson staining

Heart tissues were fixed with 4% paraformaldehyde (PFA) overnight, embedded in paraffin blocks and serial sectioned. Masson's trichrome staining was conducted to measure cardiac fibrosis. At least 6 fields per animal were randomly selected in the ventricular tissue, and six animals were studied per group. The fraction of blue stained area normalized to the total area was used as an indicator of myocardial fibrosis. Images were collected by a Leica microscope (DM6000B; Leica). ImageJ (USA) was used to analyze the results.

## 2.7. Immunofluorescence

For tissue sample immunofluorescence (IF) staining, 4% PFA-fixed hearts were paraffin-embedded and sectioned into 5  $\mu\text{m}$  thick slices. After deparaffinization and hydration, heat antigen retrieval was performed for 30 min. For cell sample IF staining, CFs were fixed with 4% PFA, treated with 0.2% Triton™ X-100 for 10 min, and blocked with blocking solution. Then, tissue slides or cells were incubated with primary antibodies overnight at 4 °C. Antibodies included anti-CD45 (1:100, #70257, Cell Signaling Technology, USA), anti-F4/80 (1:100, #70076, Cell Signaling Technology, USA), anti-IL-27 (1:500, PRS3797, Sigma), and anti-Ki67 (1:200, ab15580, Abcam). The secondary antibodies, including Alexa Fluor 488-conjugated goat anti-mouse secondary antibody (1:400, A11032, Invitrogen) and Alexa Fluor 594-conjugated goat anti-rabbit secondary antibody (1:500, A11012, Invitrogen), were incubated for 1 h at room temperature. After three washes with PBS, the slides were incubated with DAPI (4',6-diamidino-2-phenylindole) (1:100, D3571, Invitrogen) for 5 min. The immunostaining images were captured under a Leica fluorescence microscope (DM6000B, Leica, Germany). The percentage of positive cells was quantified by using ImageJ (USA), and 3–5 fields were randomly selected from each peri-infarct area in cardiac sections.

## 2.8. Cardiac fibroblast isolation and culture

CFs were isolated from neonatal C57BL/6 mice as previously described [24]. Hearts from Day 1–3 old mice were cut into small chunks. The tissue was digested with 0.25% (w/v) trypsin (Gibco) and 0.1% (w/v) collagenase II (Invitrogen) for 30 min at 37 °C 4–6 times. After centrifugation and resuspension, the single cell suspensions were plated on 100-mm culture dishes in Dulbecco's modified Eagle's medium (DMEM) with 10% fetal bovine serum (FBS) (Gibco Life Technologies, USA) for 1.5 h. Then, the nonadherent cells were washed off. The isolated CFs were cultured in DMEM with high glucose supplemented with 10% (v/v) FBS in a humidified incubator with 5% (v/v) CO<sub>2</sub> at 37 °C. The adherent cells were identified as cardiac fibroblasts. Primary cardiac fibroblasts were passaged until cells reached approximately 70%–80% confluence on the plate. The second to fourth generations of cells were used for cell treatment and further detection. The mouse cardiac fibroblast cell line was obtained from ScienCell Research Laboratories (Catalog# M6300-57), and the treatments were the same as those for primary cells.

## 2.9. Quantitative real-time polymerase chain reaction (qRT-PCR)

Cells were treated with angiotensin II (Ang II) (A9525, 1  $\mu\text{M}$ , Sigma–Aldrich) and/or mouse IL-27 recombinant protein (#RP-8611, 100 ng/ml, Invitrogen) and/or IL-27R alpha (HY-P76668, MCE) for 24 h. qRT-PCR was applied for mRNA expression analysis. Total RNA (1  $\mu\text{g}$ ) was extracted from tissue or cell sample. PrimeScript RT Reagent Kit (TaKaRa, Japan) was used to reverse mRNA to cDNA in the following system: 4  $\mu\text{l}$  of 5x PrimeScript buffer, 1  $\mu\text{g}$  of total RNA, and RNase-free deionized water were added to 20  $\mu\text{l}$ . The reverse transcription program was 15 min at 37 °C, 85 °C at 5 min, and an infinite cycle at 4 °C. A Fast Real-Time PCR System (7900HT; Applied Biosystems, Singapore) was used for qRT-PCR detection. SYBR Green MasterMix (TaKaRa, Japan) was used for RT-PCR cycling conditions. The primers that we used to detect gene expression are shown in the supplementary materials (Table S1). For example, Sample A was the control sample, and Sample B was the treated sample.  $\Delta\Delta\text{Ct} = (\text{Ct gene of interest} - \text{Ct } \beta\text{-actin})_{\text{sample B}} - (\text{Ct gene of interest} - \text{Ct } \beta\text{-actin})_{\text{sample A}}$ . Finally, relative quantification of gene expression (Sample B) =  $2^{-\Delta\Delta\text{Ct}}$ .

## 2.10. CCK-8 assay

A CCK-8 kit (Beyotime, China) was used to measure the viability of CFs, as described in the manufacturer's protocol. In brief, CFs were seeded in 96-well plates and allowed to grow overnight in 10% FBS, followed by treatment with Ang II and/or mouse IL-27 recombinant protein for 24 h. Subsequently, the supernatant was removed, and 90  $\mu\text{L}$  DMEM with 10% FBS per well was added. Thereafter, CFs were treated with 10  $\mu\text{L}$ /well CCK-8 solution in an incubator with 5% (v/v) CO<sub>2</sub> at 37 °C for 3 h. Optical density was measured with a Multiskan SkyHigh full-wavelength microplate reader (Thermo Fisher, USA) at 450 nm. The viability of CFs was defined as the absorbance of treated versus untreated control cells.

2.11. Cell migration assay

Migration of fibroblasts was measured by wound-healing assay. CFs were grown to confluence in 12-well plates, and the bottom monolayer of cells was scraped away. The remaining adhered cells were then treated with Ang II and/or mouse IL-27 recombinant protein in 1% FBS DMEM and allowed to migrate to the scraped area. At 0, 12 and 24 h, images of 5 random regions were collected from each well under an inverted microscope (DM6000B, Leica, Germany). The relative distance of CFs migration was calculated and compared with the control group.

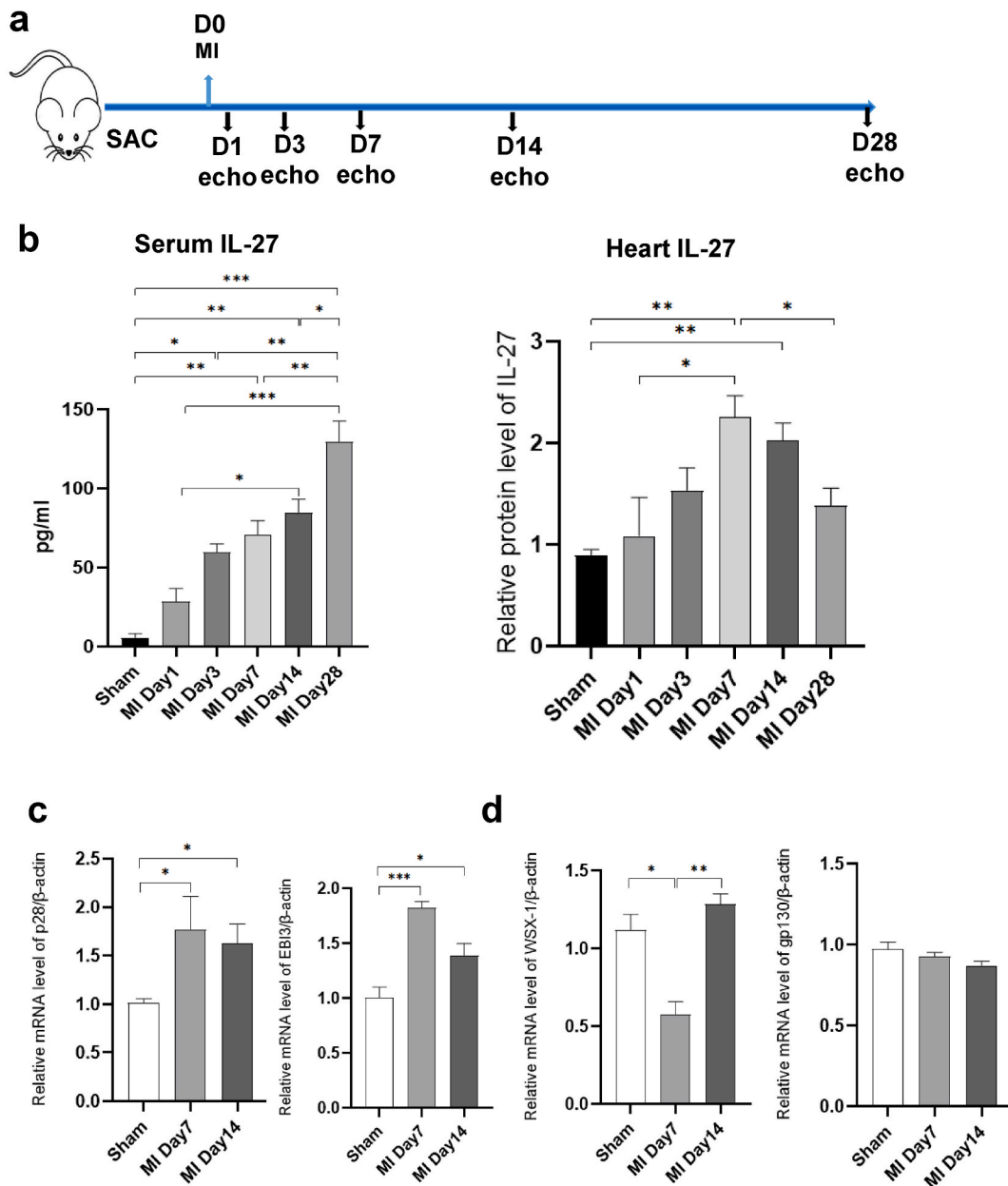


**Fig. 1.** IL-27 expression in the injured heart after MI. a) Flow chart of the experimental treatments. b) ELISA of IL-27 protein expression in serum and heart from C57BL/6 mice at various time points after MI. c) p28 and EB13 mRNA levels in the LV at 7 and 14 days after MI (n = 8). For qPCR, all data were analyzed using the 2<sup>-ΔΔCt</sup> formula. d) The expression of WSX-1 and gp130 mRNA in the LV at 7 and 14 days after MI (n = 8). All sham samples were collected at day 1 post sham operation. All data are shown as the mean ± SEM. Each experiment was repeated at least three times. \*P < 0.05; \*\*P < 0.01; \*\*\*P < 0.001 vs. sham.

## 2.12. Western blot

Cells were treated with Ang II and/or mouse IL-27 recombinant protein for 24 h. Then, cells in each group were washed with precooled PBS three times and lysed in RIPA lysis buffer (#P0013C, Beyotime) containing a protease inhibitor cocktail (Calbiochem, USA). The product was centrifuged at 13000 rpm for 15 min at 4 °C. The supernatant was obtained, and protein concentrations were determined by a BCA kit (Thermo Fisher Scientific, USA). Total protein were separated by 10% SDS-PAGE and transferred to PVDF membranes (Millipore, USA). The membranes were blocked with 5% skimmed milk for 1 h and incubated with primary antibodies overnight at 4 °C. The primary antibodies used in the study were: anti-phosphor-stat3 (1:2000, #9145, Cell signaling technology, USA), anti-stat3 (1:2000, 4904, Cell signaling technology, USA), anti- $\alpha$ -SMA (1:1000, #14968, Cell signaling technology, USA), anti-Col I (1:1000, A1352, ABclonal, USA), anti-Col III (1:1000, A0817, ABclonal, USA), anti-phosphor-JAK2 (1:1000, #4406, Cell signaling technology, USA), anti-JAK2 (1:1000, #3230, Cell signaling technology, USA) and anti- $\beta$ -actin (1:1000, #4970, Cell signaling technology, USA). The membranes were washed three times with TBS-T for 10 min each time, and then incubated with the secondary antibodies, anti-mouse IgG, HRP-linked Antibody (1:1000, #7076, Cell Signaling Technology, USA) or anti-rabbit IgG HRP-linked Antibody (1:1000, #7074, Cell Signaling Technology, USA) at room temperature for 2 h. After washing in TBS-T another three times, the bands were visualized using an enhanced chemiluminescence (ECL) system. The immune complexes were visualized by the Odyssey infrared imaging system (Li-Cor, USA).

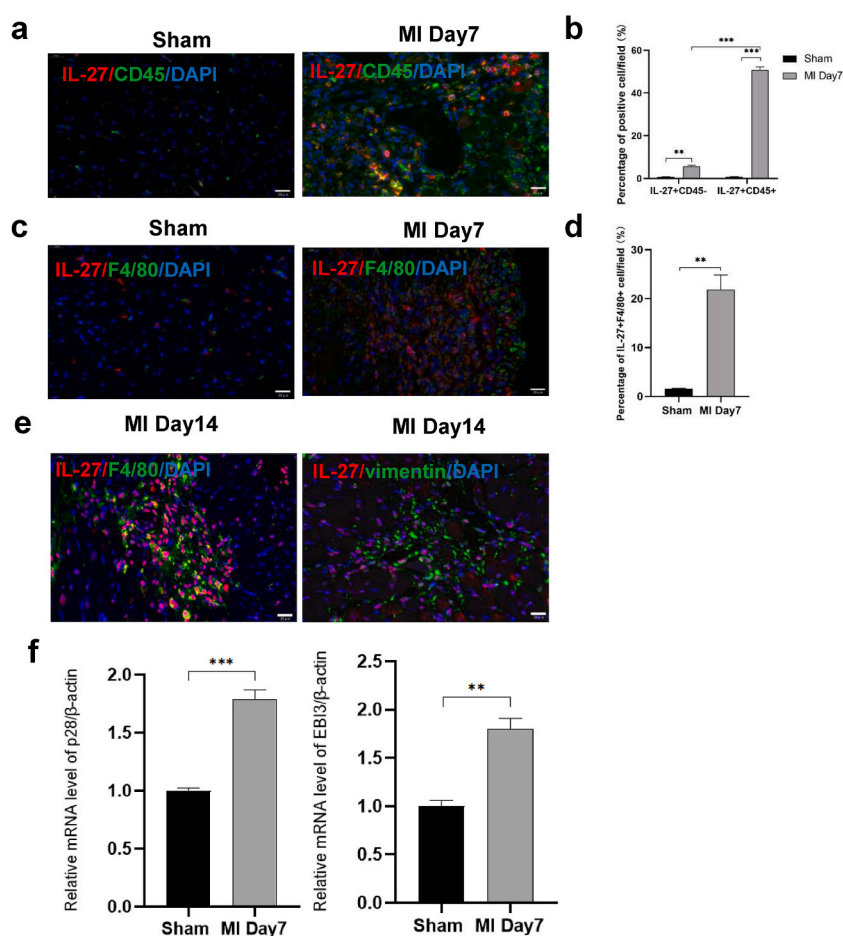


**Fig. 2.** Elevation of IL-27 in macrophages after MI. a) Representative immunofluorescence images of the expression of IL-27 (red) and CD45<sup>+</sup> (green) cells in the heart at 7 days after MI. The nuclei were stained with DAPI. Scale bar = 20  $\mu$ m. b) Quantified data of immunofluorescence images in (a). c) Representative immunofluorescence images of the expression of IL-27 (red) and F4/80<sup>+</sup> (green) cells in the heart at 7 days after MI. The nuclei were stained with DAPI. Scale bar = 20  $\mu$ m. d) Quantified data of IL-27 + F4/80<sup>+</sup> cell percentages in (c). e) Representative immunofluorescence images of the expression of IL-27 (red) and F4/80<sup>+</sup> (green) cells or vimentin<sup>+</sup> (green) cells in the heart at 14 days after MI. The nuclei were stained with DAPI. Scale bar = 20  $\mu$ m. For quantitative analysis of the immunofluorescence staining results, we counted 5 random fields in each slide. f) p28 and EB13 mRNA levels in CD45<sup>+</sup> F4/80<sup>+</sup> macrophages that were sorted by flow cytometry at 7 days after MI. Data are shown as the mean  $\pm$  SEM. Each experiment was repeated at least three times. \*P < 0.05; \*\*P < 0.01; \*\*\*P < 0.001 vs. control. (For interpretation of the references to colour in this figure legend, the reader is referred to the Web version of this article.)

### 2.13. Sorting cardiac macrophages

At day 7 after the operation, sham and MI hearts were perfused with precooled 1X PBS and collected for digestion and cell sorting. The hearts were cut into 1 mm<sup>3</sup> pieces with scissors, transferred into HBSS solution containing 1.5 mg/ml Collagenase II (Worthington) and digested on a shaker for 30 min. The digested tissue was filtered with a 70 μm filter, and Debris Removal Solution (MACS, USA) was used to defragment the heart to obtain a single-cell suspension. Next, anti-45-APC (clone 30-F11, Biolegend) and anti-F4/80-PE (clone BM8, Biolegend) were used for staining at 4 °C for 30 min. Then, CD45 + F4/80+ macrophages were sorted by fluorescence-activated cell sorting (FACS) in FACS Aria II (BD Bioscience, USA). Total RNA was extracted from these cell samples. Before qRT-PCR, ordinary PCR preamplification was performed, and the products were used as templates for qRT-PCR.

### 2.14. Statistical analysis

All the data are presented as the means ± S.E.M.s for at least five independent assays unless otherwise noted. All data were evaluated for normality and equal variance before analysis. Data were analyzed by SPSS 11.0 (SPSS Inc., USA) statistical software and GraphPad Prism 8 statistical software (GraphPad Software Inc., San Diego, California). One-way ANOVA with Tukey post hoc tests was used for comparisons between multiple groups, and two-way ANOVA was used for comparisons between multiple groups when there were two experimental factors. P values of less than 0.05 were considered statistically significance.

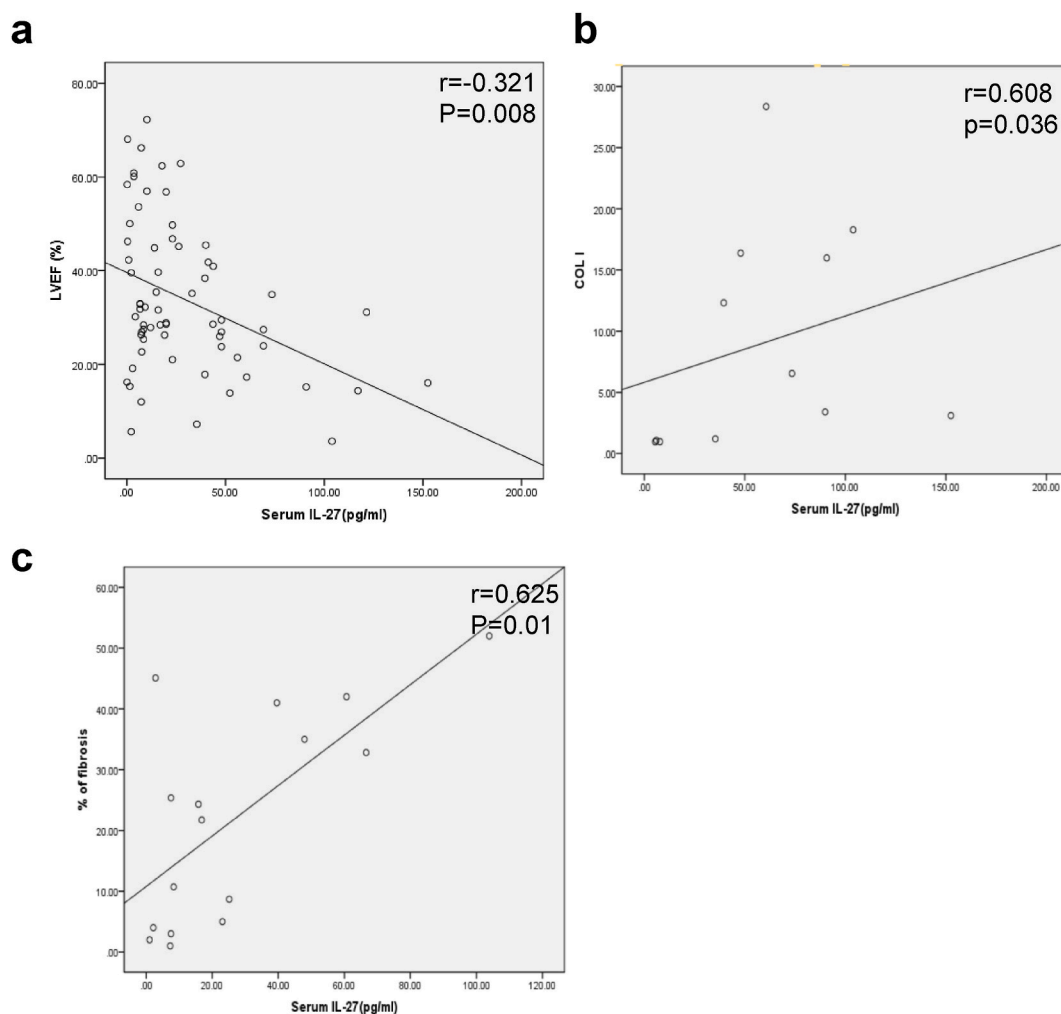


**Fig. 3.** The expression of IL-27 in serum is associated with cardiac function and cardiac fibrosis. a) Serum IL-27 was significantly associated with LVEF after MI. b) Serum IL-27 was significantly correlated with heart Col I mRNA expression after MI. c) Serum IL-27 was significantly associated with the area of cardiac fibrosis by Masson staining after MI. For quantitative analysis of the Masson staining, we counted six random fields of each slide for each mouse. The percentage of the fibrosis area (blue) in each section was calculated by ImageJ software. Data are expressed as the mean ± SEM. \* $P < 0.05$ ; \*\* $P < 0.01$ ; \*\*\* $P < 0.001$ .

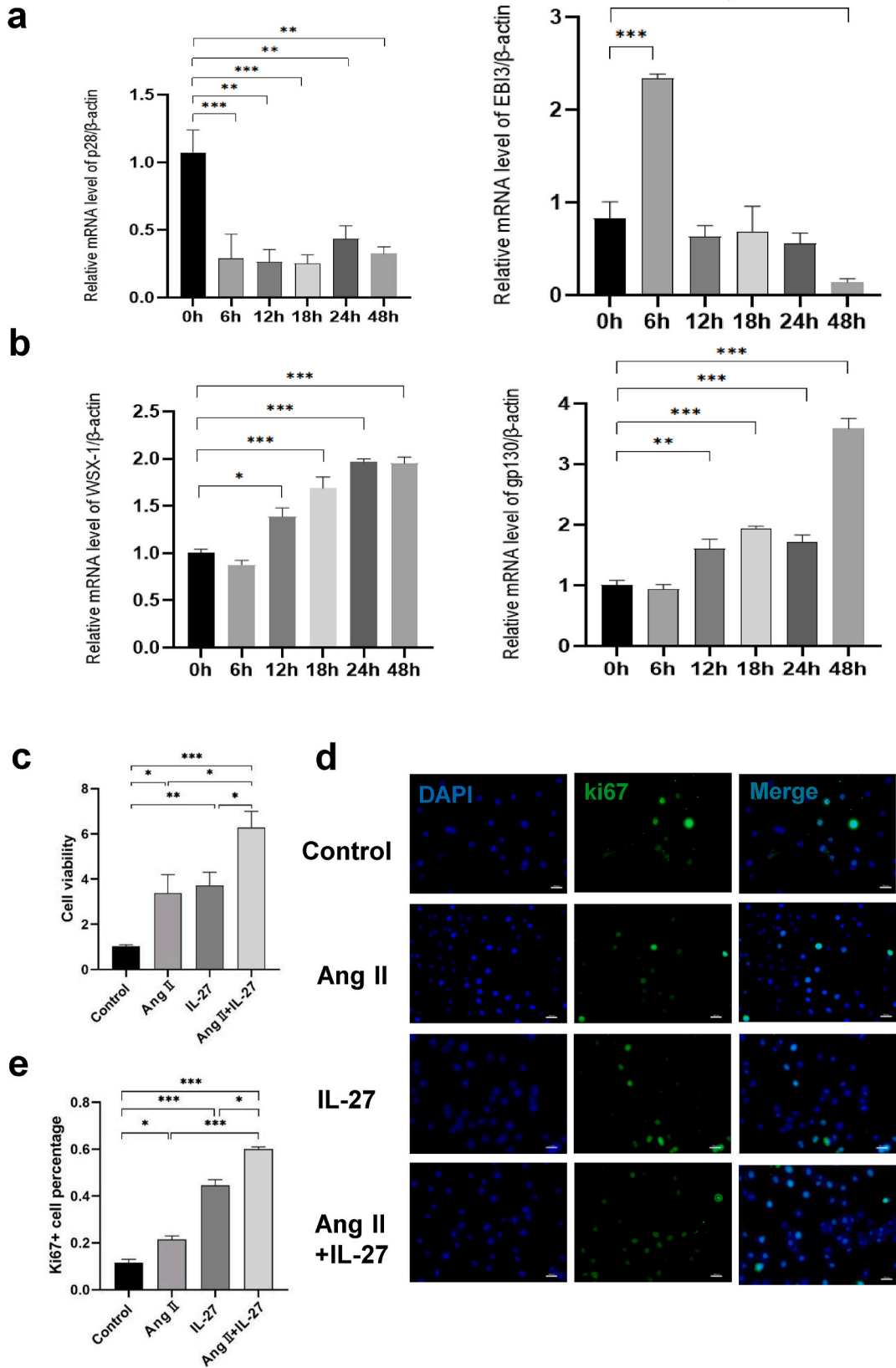


**Fig. 4.** Effect of IL-27 on the proliferation and migration of cardiac fibroblasts induced by Ang II. a) The mRNA expression of p28 and EBI3 in cardiac fibroblasts treated with Ang II (1  $\mu$ m) for 0, 6, 12, 18, 24, and 48 h. b) The mRNA expression of WSX-1 and gp130 in cardiac fibroblasts treated with Ang II (1  $\mu$ m) for 0, 6, 12, 18, 24, and 48 h. c) Cell viability of cardiac fibroblasts was measured in different groups by CCK-8 assay. d) Representative immunofluorescence images of the expression of Ki67 (green) protein in different groups. The nuclei were stained with DAPI. Scale bar = 200  $\mu$ m. e) Statistical results of Ki67+ cell percentages in (d). f) Cell migration distance in different groups at 12 or 24 h after scratching. g) Quantification of scratch widths in separate experiments at 12 h. Wound closure distance (%) = [(the initialized width of the scratch) - (the final width of the scratch)]/(the initialized width of the scratch). h) Quantification of scratch widths in separate experiments at 24 h. The images used for the statistics are the six random fields of the scratch widths captured for statistics. Values are the mean  $\pm$  SEM from at least three experiments. \*P < 0.05; \*\*P < 0.01; \*\*\*P < 0.001 vs. control. (For interpretation of the references to colour in this figure legend, the reader is referred to the Web version of this article.)

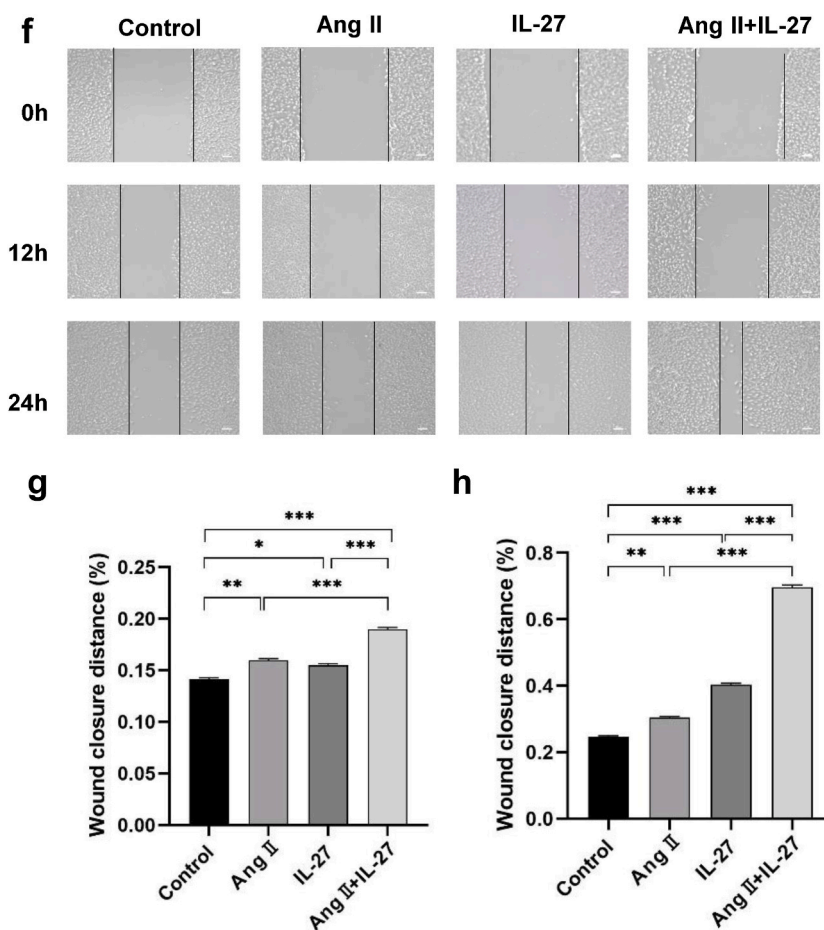


**Fig. 4.** (continued).

### 3. Results

#### 3.1. The expression of IL-27 increased in the injured heart post MI

Our previous study found high levels of IL-27 protein in the heart on days 7 and 14 post MI/R [20]. We further evaluated the dynamic change in IL-27 in ischemic heart tissues and serum. Fig. 1(a) shows the flow chart of the treatment. IL-27 protein level in serum gradually increased post MI, and significantly upregulated at day7, day14, and day28, compared with that in the sham group (Fig. 1(b)). Cardiac IL-27 protein level also increased on day7 and day14, compared to that in sham heart (Fig. 1(b)). In addition, compared with the sham group, the mRNA expressions of both p28 and EBI3, two subunits of IL-27, significantly increased in the heart on day7 and day14 (Fig. 1(c)).

IL-27 exerts its effect by binding to its receptors. We further assessed the expression of IL-27 receptor subunits, including WSX-1 and gp130, in the heart after MI. As shown in Fig. 1(d), the mRNA level of WSX-1 decreased dramatically on day 7 compared to the sham group but increased on day 14 compared to day 7 after MI. There was no significant change in gp130 mRNA levels between these groups.

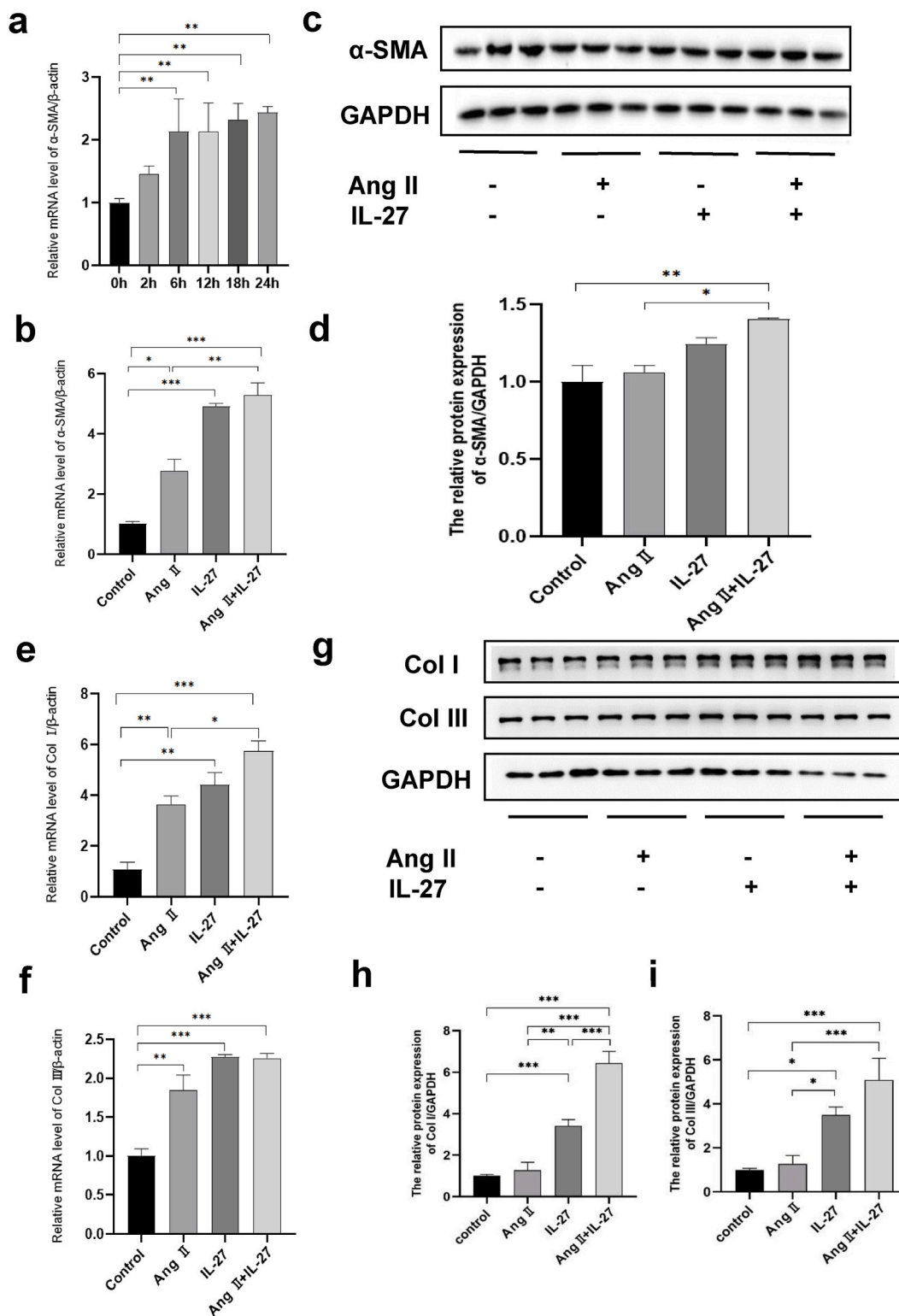


**Fig. 5.** Effect of IL-27 on the differentiation of CFs to myofibroblasts and ECM production induced by Ang II. a) α-SMA mRNA expression in cardiac fibroblasts after treatment with IL-27 (100 ng/ml) for 0, 2, 6, 12, 18, and 24 h. b) α-SMA mRNA levels in cardiac fibroblasts treated with different conditions for 24 h. c) Western blotting was used to analyze the protein level of α-SMA in cardiac fibroblasts in different groups. d) The results were quantified using ImageJ software. e) Col I mRNA expression in cardiac fibroblasts in different groups. f) Col III mRNA expression in cardiac fibroblasts in different groups. g) Western blotting was used to analyze the protein levels of Col I and Col III in cardiac fibroblasts in different groups.

h-i) Col I and Col III mRNA expression in cardiac fibroblasts in different groups. All data are shown as the mean ± SEM. Each experiment was repeated at least three times. \*P < 0.05; \*\*P < 0.01; \*\*\*P < 0.001 vs. control.

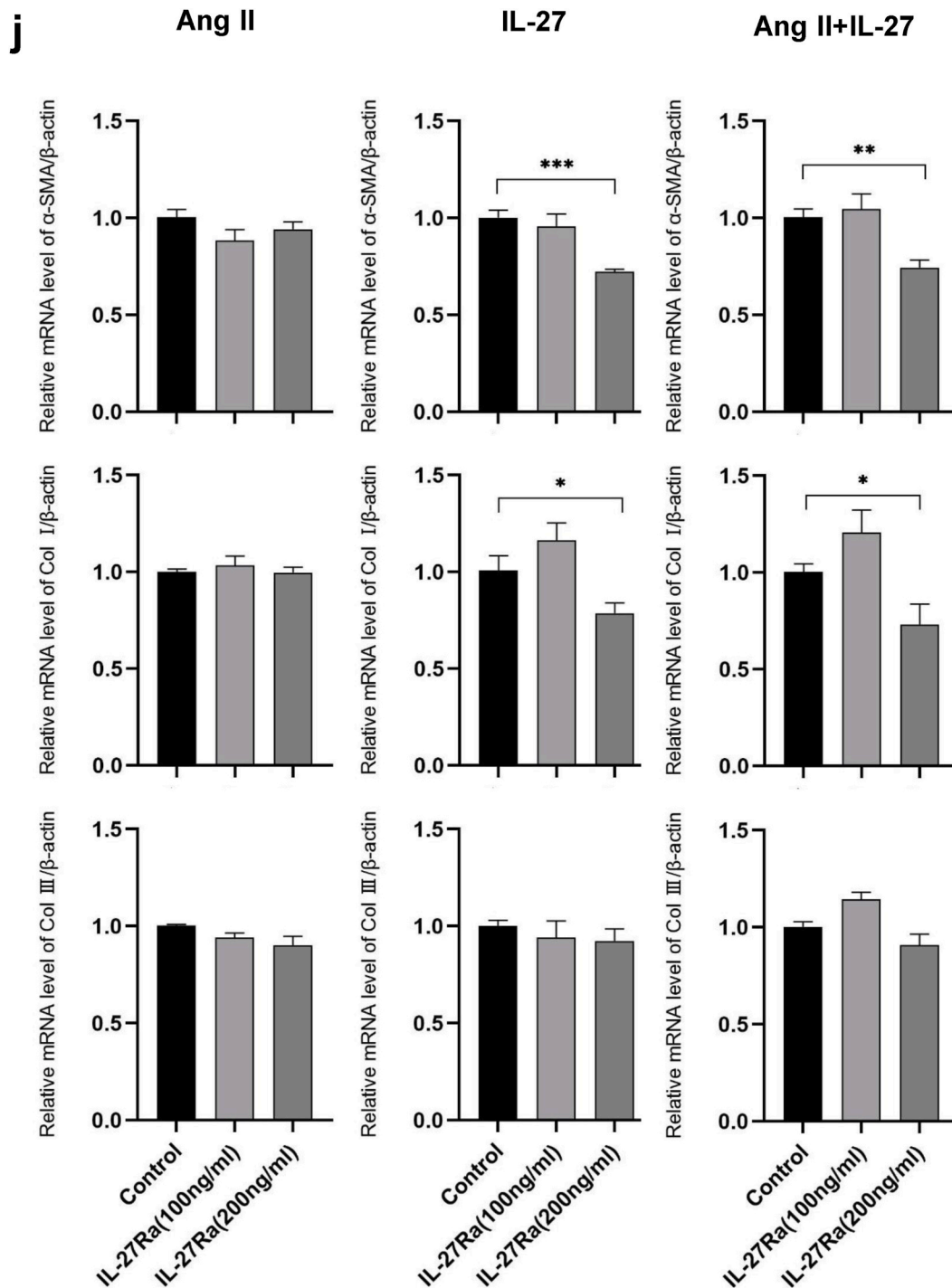
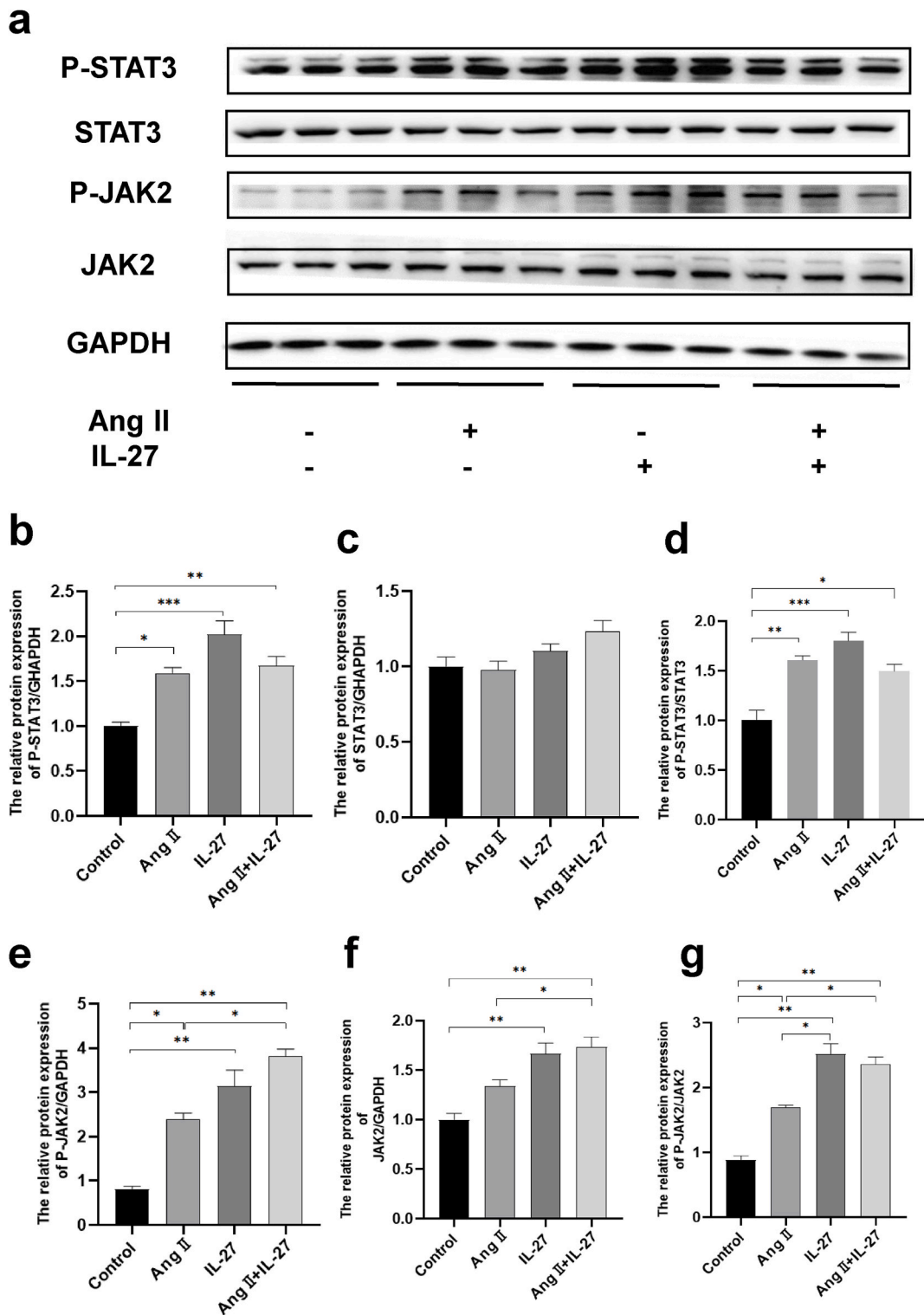


Fig. 5. (continued).

### 3.2. MI triggered the elevation of IL-27 in cardiac macrophages

Previous studies confirmed that myocardial infarction elicits an inflammatory response that plays a key role in myocardial repair and remodeling [25]. The infiltration of immune cells, especially macrophages, represents the major immune cell subtype in this



**Fig. 6.** IL-27 promotes the activation of the JAK/STAT3 signaling pathway in Ang II-induced CFs. a) Western blotting was used to analyze the protein levels of P-JAK2, JAK2, P-STAT3, and STAT3 in cardiac fibroblasts in different groups. b-g) Quantified data of immunoblotting band intensity in A. All data are shown as the mean  $\pm$  SEM from at least three experiments. \* $P < 0.05$ ; \*\* $P < 0.01$ ; \*\*\* $P < 0.001$  vs. control.

process [26]. Moreover, IL-27 was reported to be produced mainly by activated APCs [27]. We next examined the expression of IL-27 in immune cells with the surface marker CD45 and macrophages with F4/80. Fig. 2(a) shows the proportion of IL-27-positive cells in different cell types in the heart after MI via IF staining. Although the percentage of IL-27 + CD45<sup>-</sup> cells increased in MI hearts compared to sham hearts, we found a large number of CD45<sup>+</sup> immune cells expressing IL-27 in injured hearts (Fig. 2(b)). Further results showed that cardiac F4/80<sup>+</sup> cells displayed high levels of IL-27 after MI (Fig. 2(c) and (d)), while IL-27 could not be observed in vimentin-positive fibroblasts (Fig. 2(e)). In CD45 + F4/80<sup>+</sup> macrophages sorted from the hearts, the mRNA expressions of both p28 and EB13 were significantly elevated in the MI group compared to the sham group at day 7 (Fig. 2(f)). Therefore, the elevation of IL-27 levels is mainly attributed to cardiac macrophages after MI.

### 3.3. Negative correlation of serum IL-27 level with cardiac function and fibrosis after MI

Next, we determined whether high levels of serum IL-27 are related to cardiac function and fibrosis post MI. As shown in Fig. 3(a), serum IL-27 protein expression on days 0, 1, 3, 7, 14, and 28 was negatively correlated with the LVEF ( $r = -0.321$ ;  $p = 0.008$ ). Fig. 3(b) revealed that serum IL-27 protein levels were positively correlated with Col I mRNA expression on days 7 and 14 ( $r = 0.608$ ;  $p = 0.036$ ). Moreover, serum IL-27 was positively correlated with the area of fibrosis shown by Masson staining at day 14 ( $r = 0.625$ ;  $p = 0.01$ , Fig. 3(c)). Therefore, high levels of IL-27 in serum may reflect the deterioration of cardiac function and cardiac fibrosis to some degree after MI in murine models.

### 3.4. IL-27 promoted the proliferation and migration of cardiac fibroblasts induced by Ang II

CFs play important roles in cardiac fibrosis and ventricular remodeling after MI [28]. Ang II is generally used to establish a cell model to mimic the proliferation and migration of cardiac fibroblasts after MI [24]. Then, we treated cardiac fibroblasts with Ang II, IL-27 or both to explore the effect of IL-27 on CFs. First, p28 expression in CFs was downregulated until 48 h, while the EB13 level increased at 6 h and then decreased upon Ang II treatment (Fig. 4(a)). Compared with the control group, Ang II treatment significantly increased both IL-27 receptors in cardiac fibroblasts from 12 h to 48 h (Fig. 4(b)). Next, the viability results revealed that either Ang II or IL-27 alone increased the cell viability, while IL-27 further promoted the increase in cell viability induced by Ang II (Fig. 4(c)). IF staining of Ki67 showed results similar to those of CCK-8 assays (Fig. 4(d) and (e)). In addition, the scratch wound assay showed that Ang II or IL-27 alone promoted the migration of CFs at 12 h and 24 h, while IL-27 further promoted the migration of CFs with Ang II treatment (Fig. 4(f), (g), and 4(h)). Hence, the addition of IL-27 can promote the proliferation and migration of Ang II-induced CFs.

### 3.5. IL-27 contributed to the differentiation of CFs to myofibroblasts and ECM production induced by Ang II

After MI, CFs are activated and differentiated into myofibroblasts [29], contributing to cardiac fibrosis. To detect whether IL-27 exerts its role in this process, CFs were treated with Ang II and/or mouse IL-27 recombinant protein for 2–24 h (Fig. 5(a)). We found that the addition of IL-27 to Ang II-treated cells enhanced both the mRNA and protein expression of  $\alpha$ -SMA (Fig. 5(b–d)).

Excessive accumulation of ECM is vital for cardiac remodeling after MI [30]. Then, we analyzed the expression of Col I and Col III in CFs with different treatments. Fig. 5(e) and (f) show that both Col I and Col III mRNA expression increased markedly in the IL-27 group compared to the control. When compared with the Ang II-induced group, the addition of IL-27 significantly enhanced the expression of Col I (Fig. 5(e)). Further Western blot results revealed that compared to the control group, both Col I and Col III in CFs tended to increase when treated with Ang II and significantly increased in the IL-27 treatment group. In addition, compared to those in the Ang II group, the protein levels of Col I and Col III were markedly upregulated in CFs treated with Ang II and IL-27 (Fig. 5(g–i)). Likewise, IL-27 also increased Col I and Col III expression in CFs treated with transforming growth factor-beta (TGF- $\beta$ 1) (Figure s1). Taken together, these results suggested that IL-27 can promote Ang II-induced ECM deposition of CFs.

Next, we determined whether blockade of IL-27 signaling can reverse the effect of Ang II. An IL-27 receptor antagonist (100 and 200 ng/ml) was added to CFs treated with Ang II and/or IL-27 for 24 h. As shown in Fig. 5(j), neither 100 ng/ml nor 200 ng/ml IL-27 receptor antagonist affected the expression of  $\alpha$ -SMA, Col I and Col III in Ang II-induced CFs. The block of IL-27 signaling via receptor antagonists cannot reverse the effects of Ang II in CFs. Administration of 200 ng/ml IL-27 receptor antagonist reduced the mRNA expression of  $\alpha$ -SMA and Col I in both IL-27-induced CFs and Ang II + IL-27-treated CFs. These results suggested that IL-27 signaling can exert its role on CFs with or without Ang II treatment.

### 3.6. IL-27 promotes the activation of the JAK/STAT signaling pathway in Ang II-induced CFs

A previous study showed that JAK/STAT is one of the important signaling pathways mediating cardiac remodeling [31]. Of note, Ang II enhanced the activity of the JAK/STAT signal transduction pathway in all cardiac cells, including cardiomyocytes and CFs [32, 33]. We next determined whether the addition of IL-27 affected this pathway in CFs. As shown in Fig. 6(a) and (b), 6(c) and 6(d), IL-27 alone upregulated the phosphorylation of STAT3 and increased the ratio of phosphorylated STAT3 (P-STAT3) to total STAT3 in CFs compared to the control cells after 24 h. Cells treated with IL-27 after 24 h also showed higher phosphorylated JAK2 (P-JAK2) and a higher ratio of P-JAK2 to total JAK2 compared to the control (Fig. 6(e), (f), and 6(g)). Compared to the Ang II group, the addition of IL-27 increased the ratio of P-JAK2 to total JAK2 (Fig. 6(g)). These results indicated that IL-27 can activate the JAK/STAT signaling pathway in both untreated CFs and Ang II-treated cells.

#### 4. Discussion

Chronic inflammation plays a vital role in cardiac remodeling post MI. In the present study, we found that MI triggered high IL-27 expression in cardiac macrophages. The increased IL-27 protein level in serum is correlated with cardiac dysfunction and fibrosis in murine MI models. Moreover, IL-27 treatment contributed to the activation of the JAK/STAT signaling pathway in CFs and promoted their differentiation into myofibroblasts and ECM deposition.

A previous clinical study reported the upregulation of IL-27 levels in the serum of patients with ischemic heart disease during the acute period (3–5 days for acute MI patients after events and admission time for unstable angina) [19]. In murine MI/R models, we found that IL-27 levels in serum and heart tissue were significantly increased until day 14 [20]. Furthermore, we demonstrated that the elevation of serum IL-27 was maintained until day 28 after MI, suggesting that high IL-27 levels in serum may be involved in cardiac healing and remodeling at the chronic stage.

IL-27 is produced primarily by APCs, including monocytes, macrophages, and DCs [34]. Macrophages represent the major infiltrating cell types in the heart after MI [35,36]. A previous study revealed that the elevation of IL-27 protein in carotid plaques is localized in macrophages [37]. In this study, we found a significant increase in IL-27 in F4/80+ macrophages in the infarcted heart but not in CFs, indicating that the elevation of IL-27 protein may be mainly attributed to cardiac macrophages after MI.

Previously, two clinical studies showed the correlations between IL-27 level and the disease progress [21,38]; one showed the associations between IL-27 levels at baseline and parameters of left ventricular remodeling, systolic and diastolic function in 107 patients who underwent echocardiographic control examinations at 1 year after the acute event [38]. In these patients, baseline IL-27 is associated negatively with LVEF at 1 year, while elevated baseline IL-27 levels were associated with accelerated LV remodeling, as indicated by increased parameters of left ventricular dilation and hypertrophy at 1 year follow-up [38]. In another study, serum IL-27 levels were positively correlated with the extent of skin fibrosis in patients with systemic sclerosis [21]. In the present study, we found a significant negative correlation of serum IL-27 levels with cardiac function. Moreover, serum IL-27 levels were positively correlated with Col I and fibrosis area in murine MI models. These results indicated that high IL-27 levels may be used to predict cardiac dysfunction and fibrosis post MI. Further clinical cohorts are needed to evaluate its clinical translational value in patients.

Macrophages after activation can stimulate the inflammatory program of cardiac fibroblasts [36,39]. Overactivation of macrophages can secrete a variety of inflammatory factors and promote the differentiation of cardiac fibroblasts into myofibroblasts [40,41]. A previous study showed that IL-27 can attenuate proliferation, differentiation, and collagen synthesis in TGF- $\beta$ 1-induced lung fibroblasts [42]. Another study reported that IL-27 stimulation increased proliferation and collagen synthesis in the fibroblasts of patients with systemic sclerosis compared to those of healthy controls [21]. The present results showed that IL-27 could promote the differentiation of CFs and contribute to their collagen formation. Distinct from the TGF- $\beta$ 1-induced lung fibrosis models, we mainly used Ang II to mimic the fibrosis cell model in CFs. We also found that IL-27 augments Col I and Col III mRNA expression in CFs treated with TGF- $\beta$ 1. Thus, IL-27 may play diverse roles in different cell types and models. How IL-27 affects the pathology of fibrosis in other organs requires further exploration. Activated myofibroblasts are the main source of structural ECM proteins in fibrotic hearts [43]. Therefore, high levels of IL-27 in infarcted hearts promote the collagen production of CFs and aggravate cardiac fibrosis post MI. Further studies are needed to confirm the effect of IL-27-related interventions on cardiac fibrosis in vivo.

Previous studies have shown that IL-27 can regulate cellular function via multiple signaling pathways, including the JAK/STAT and p38 MAPK pathways [44]. Among them, the JAK/STAT signaling pathway is a key pathway involved in fibrosis [45]; it also modulates the functions of fibroblasts and promotes the differentiation of fibroblasts into myofibroblasts [46]. In addition, activation of JAK/STAT signaling by Ang II contributes to cardiac dysfunction during ischemia and heart failure [47,48]. A previous study revealed that Ang II can promote the upregulation of  $\alpha$ -SMA and collagen expression by activating the JAK/STAT signaling pathway [49]. Stat3 is a member of the STAT protein family, and its phosphorylation at Tyr705 is involved in CFs activation and cardiac fibrosis [50]. Then, we assessed the expression of phosphorylated JAK2 and Stat3 in CFs under different conditions. We found that either IL-27 or Ang II upregulated the ratio of P-STAT3/STAT3, while the addition of IL-27 further upregulated P-JAK2/JAK2 in Ang II-treated CFs. We also found that IL-27 significantly promoted the expression of  $\alpha$ -SMA and the formation of collagen in Ang II-treated CFs (Fig. 5). These results suggested that a high level of IL-27 not only exerts its role independently but also functions with Ang II synthetically by activating the JAK/STAT signaling pathway, contributing to cardiac fibrosis post MI.

#### 5. Conclusion

In summary, high levels of IL-27 mainly produced by cardiac macrophages promoted the collagen production of CFs and aggravated cardiac fibrosis in murine MI models. These findings provide a potential target for prevention and alleviation of cardiac fibrosis and ventricular remodeling after MI.

#### Author contribution statement

Xiaoxue Ma: Performed the experiments, Analyzed and interpreted the data, Contributed reagents, materials, analysis tools or data, Wrote the paper.

Qingshu Meng, Shiyu Gong, Shanshan Shi, Li Gong, Xuan Liu: Performed the experiments.

Xiaoting Liang, Fang Lin, Yinzheng Li, Mimi Li, Lu Wei, Leng Gao: Contributed reagents, materials, analysis tools or data. Wei Han: Analyzed and interpreted the data.

Zhongmin Liu, Xiaohui Zhou: Conceived and designed the experiments.

## Funding statement

The study was supported by the National Key Research and Development Program of China (2017YFA0105600), the National Natural Science Foundation of China (81670458), Shanghai Engineering Research Center of Artificial Heart and Heart Failure Medicine (grant no. 19DZ2251000), Major Program of Development Fund for Shanghai Zhangjiang National Innovation Demonstration Zone (grant no. ZJ2018-ZD-004) and Peak Disciplines (Type IV) of Institutions of Higher Learning in Shanghai.

## Data availability statement

No data was used for the research described in the article.

## Declaration of competing interest

The authors declare that they have no known competing financial interests or personal relationships that could have appeared to influence the work reported in this paper.

## Appendix A. Supplementary data

Supplementary data to this article can be found online at <https://doi.org/10.1016/j.heliyon.2023.e17099>.

## References

- [1] B. Li, H. Yang, X. Wang, Y. Zhan, W. Sheng, H. Cai, H. Xin, Q. Liang, P. Zhou, C. Lu, R. Qian, S. Chen, P. Yang, J. Zhang, W. Shou, G. Huang, P. Liang, N. Sun, Engineering human ventricular heart muscles based on a highly efficient system for purification of human pluripotent stem cell-derived ventricular cardiomyocytes, *Stem Cell Res. Ther.* 8 (1) (2017) 202.
- [2] M. Jung, Y. Ma, R.P. Iyer, K.Y. DeLeon-Pennell, A. Yabluchanskiy, M.R. Garrett, M.L. Lindsey, IL-10 improves cardiac remodeling after myocardial infarction by stimulating M2 macrophage polarization and fibroblast activation, *Basic Res. Cardiol.* 112 (3) (2017) 33.
- [3] S.B. Ong, S. Hernandez-Resendiz, G.E. Crespo-Avilan, R.T. Mukhametshina, X.Y. Kwek, H.A. Cabrera-Fuentes, D.J. Hausenloy, Inflammation following acute myocardial infarction: multiple players, dynamic roles, and novel therapeutic opportunities, *Pharmacol. Ther.* 186 (2018) 73–87.
- [4] X. Yan, H. Zhang, Q. Fan, J. Hu, R. Tao, Q. Chen, Y. Iwakura, W. Shen, L. Lu, Q. Zhang, R. Zhang, Dectin-2 deficiency modulates Th1 differentiation and improves wound healing after myocardial infarction, *Circ. Res.* 120 (7) (2017) 1116–1129.
- [5] S. McLaughlin, B. McNeill, J. Podrebarac, K. Hosoyama, V. Sedlakova, G. Cron, D. Smyth, R. Seymour, K. Goel, W. Liang, K.J. Rayner, M. Ruel, E.J. Suuronen, E. I. Alarcon, Injectable human recombinant collagen matrices limit adverse remodeling and improve cardiac function after myocardial infarction, *Nat. Commun.* 10 (1) (2019) 4866.
- [6] N.G. Frangogiannis, The inflammatory response in myocardial injury, repair, and remodeling, *Nat. Rev. Cardiol.* 11 (5) (2014) 255–265.
- [7] Q.Q. Wu, Y. Xiao, Y. Yuan, Z.G. Ma, H.H. Liao, C. Liu, J.X. Zhu, Z. Yang, W. Deng, Q.Z. Tang, Mechanisms contributing to cardiac remodeling, *Clin. Sci. (Lond.)* 131 (18) (2017) 2319–2345.
- [8] N.G. Frangogiannis, The immune system and the remodeling infarcted heart: cell biological insights and therapeutic opportunities, *J. Cardiovasc. Pharmacol.* 63 (3) (2014) 185–195.
- [9] N.G. Frangogiannis, The immune system and cardiac repair, *Pharmacol. Res.* 58 (2) (2008) 88–111.
- [10] R.A. Frieler, R.M. Mortensen, Immune cell and other noncardiomyocyte regulation of cardiac hypertrophy and remodeling, *Circulation* 131 (11) (2015) 1019–1030.
- [11] X. Yan, A. Anzai, Y. Katsumata, T. Matsushashi, K. Ito, J. Endo, T. Yamamoto, A. Takeshima, K. Shinmura, W. Shen, K. Fukuda, M. Sano, Temporal dynamics of cardiac immune cell accumulation following acute myocardial infarction, *J. Mol. Cell. Cardiol.* 62 (2013) 24–35.
- [12] C. Peet, A. Ivetic, D.I. Bromage, A.M. Shah, Cardiac monocytes and macrophages after myocardial infarction, *Cardiovasc. Res.* 116 (6) (2020) 1101–1112.
- [13] G. de Couto, W. Liu, E. Tselioui, B. Sun, N. Makkar, H. Kanazawa, M. Arditi, E. Marban, Macrophages mediate cardioprotective cellular postconditioning in acute myocardial infarction, *J. Clin. Invest.* 125 (8) (2015) 3147–3162.
- [14] J.P. Cleutjens, M.J. Verluyten, J.F. Smiths, M.J. Daemen, Collagen remodeling after myocardial infarction in the rat heart, *Am. J. Pathol.* 147 (2) (1995) 325–338.
- [15] L. Li, Q. Zhao, W. Kong, Extracellular matrix remodeling and cardiac fibrosis, *Matrix Biol.* 68–69 (2018) 490–506.
- [16] S. Pflanz, J.C. Timans, J. Cheung, R. Rosales, H. Kanzler, J. Gilbert, L. Hibbert, T. Churakova, M. Travis, E. Vaisberg, W.M. Blumenschein, J.D. Mattson, J. L. Wagner, W. To, S. Zurawski, T.K. McClanahan, D.M. Gorman, J.F. Bazan, R. de Waal Malefyt, D. Rennick, R.A. Kastelein, IL-27, a heterodimeric cytokine composed of EB13 and p28 protein, induces proliferation of naive CD4+ T cells, *Immunity* 16 (6) (2002) 779–790.
- [17] J. Ye, Y. Wang, Z. Wang, L. Liu, Z. Yang, M. Wang, Y. Xu, D. Ye, J. Zhang, Y. Lin, Q. Ji, J. Wan, Roles and mechanisms of interleukin-12 family members in cardiovascular diseases: opportunities and challenges, *Front. Pharmacol.* 11 (2020) 129.
- [18] C. Andrews, M.H. McLean, S.K. Durum, Interleukin-27 as a novel therapy for inflammatory bowel disease: a critical review of the literature, *Inflamm. Bowel Dis.* 22 (9) (2016) 2255–2264.
- [19] A. Jafarzadeh, M. Nemati, M.T. Rezayati, Serum levels of interleukin (IL)-27 in patients with ischemic heart disease, *Cytokine* 56 (2) (2011) 153–156.
- [20] D. Yuan, J. Tie, Z. Xu, G. Liu, X. Ge, Z. Wang, X. Zhang, S. Gong, G. Liu, Q. Meng, F. Lin, Z. Liu, H. Fan, X. Zhou, Dynamic profile of CD4(+) T-cell-associated cytokines/chemokines following murine myocardial infarction/reperfusion, *Mediat. Inflamm.* 2019 (2019), 9483647.
- [21] A. Yoshizaki, K. Yanaba, Y. Iwata, K. Komura, A. Ogawa, E. Muroi, F. Ogawa, M. Takenaka, K. Shimizu, M. Hasegawa, M. Fujimoto, S. Sato, Elevated serum interleukin-27 levels in patients with systemic sclerosis: association with T cell, B cell and fibroblast activation, *Ann. Rheum. Dis.* 70 (1) (2011) 194–200.
- [22] X. Liang, Y. Ding, Y. Zhang, Y.H. Chai, J. He, S.M. Chiu, F. Gao, H.F. Tse, Q. Lian, Activation of NRG1-ERBB4 signaling potentiates mesenchymal stem cell-mediated myocardial repairs following myocardial infarction, *Cell Death Dis.* 6 (2015) e1765.
- [23] J. Liu, T. Zhuang, J. Pi, X. Chen, Q. Zhang, Y. Li, H. Wang, Y. Shen, B. Tomlinson, P. Chan, Z. Yu, Y. Cheng, X. Zheng, M. Reilly, E. Morrissey, L. Zhang, Z. Liu, Y. Zhang, Endothelial forkhead box transcription factor P1 regulates pathological cardiac remodeling through transforming growth factor-beta1-endothelin-1 signal pathway, *Circulation* 140 (8) (2019) 665–680.
- [24] X. Tao, J. Fan, G. Kao, X. Zhang, L. Su, Y. Yin, B. Zrenner, Angiotensin-(1-7) attenuates angiotensin II-induced signalling associated with activation of a tyrosine phosphatase in Sprague-Dawley rats cardiac fibroblasts, *Biol. Cell.* 106 (6) (2014) 182–192.

- [25] I. Kologrivova, M. Shtatolkin, T. Suslova, V. Ryabov, Cells of the immune system in cardiac remodeling: main players in resolution of inflammation and repair after myocardial infarction, *Front. Immunol.* 12 (2021), 664457.
- [26] A. Moskalik, J. Niderla-Bielinska, A. Ratajska, Multiple roles of cardiac macrophages in heart homeostasis and failure, *Heart Fail. Rev.* 27 (4) (2022) 1413–1430.
- [27] S. Pflanz, L. Hibbert, J. Mattson, R. Rosales, E. Vaisberg, J.F. Bazan, J.H. Phillips, T.K. McClanahan, R. de Waal Malefyt, R.A. Kastelein, WSX-1 and glycoprotein 130 constitute a signal-transducing receptor for IL-27, *J. Immunol.* 172 (4) (2004) 2225–2231.
- [28] N.G. Frangogiannis, Cardiac fibrosis: cell biological mechanisms, molecular pathways and therapeutic opportunities, *Mol. Aspect. Med.* 65 (2019) 70–99.
- [29] N.G. Frangogiannis, Pathophysiology of myocardial infarction, *Compr. Physiol.* 5 (4) (2015) 1841–1875.
- [30] S.W. van den Borne, J. Diez, W.M. Blankesteyn, J. Verjans, L. Hofstra, J. Narula, Myocardial remodeling after infarction: the role of myofibroblasts, *Nat. Rev. Cardiol.* 7 (1) (2010) 30–37.
- [31] S.P. Barry, P.A. Townsend, D.S. Latchman, A. Stephanou, Role of the JAK-STAT pathway in myocardial injury, *Trends Mol. Med.* 13 (2) (2007) 82–89.
- [32] M.B. Marrero, B. Schieffer, W.G. Paxton, L. Heerdt, B.C. Berk, P. Delafontaine, K.E. Bernstein, Direct stimulation of Jak/STAT pathway by the angiotensin II AT1 receptor, *Nature* 375 (6528) (1995) 247–250.
- [33] E. Mascareno, M. Dhar, M.A. Siddiqui, Signal transduction and activator of transcription (STAT) protein-dependent activation of angiotensinogen promoter: a cellular signal for hypertrophy in cardiac muscle, *Proc. Natl. Acad. Sci. U. S. A.* 95 (10) (1998) 5590–5594.
- [34] C.A. Hunter, New IL-12-family members: IL-23 and IL-27, cytokines with divergent functions, *Nat. Rev. Immunol.* 5 (7) (2005) 521–531.
- [35] S.D. Prabhu, N.G. Frangogiannis, The biological basis for cardiac repair after myocardial infarction: from inflammation to fibrosis, *Circ. Res.* 119 (1) (2016) 91–112.
- [36] P.C. Schulze, R.T. Lee, Macrophage-mediated cardiac fibrosis, *Circ. Res.* 95 (6) (2004) 552–553.
- [37] A.J. Shih, A. Menzin, J. Whyte, J. Lovecchio, A. Liew, H. Khalili, T. Bhuiya, P.K. Gregersen, A.T. Lee, Correction: identification of grade and origin specific cell populations in serous epithelial ovarian cancer by single cell RNA-seq, *PLoS One* 13 (12) (2018), e0208778.
- [38] H. Grufman, T. Yndigeñ, I. Goncalves, J. Nilsson, A. Schiopu, Elevated IL-27 in patients with acute coronary syndrome is associated with adverse ventricular remodeling and increased risk of recurrent myocardial infarction and cardiovascular death, *Cytokine* 122 (2019), 154208.
- [39] M. Hulsmans, F. Sam, M. Nahrendorf, Monocyte and macrophage contributions to cardiac remodeling, *J. Mol. Cell. Cardiol.* 93 (2016) 149–155.
- [40] D. Jia, H. Jiang, X. Weng, J. Wu, P. Bai, W. Yang, Z. Wang, K. Hu, A. Sun, J. Ge, Interleukin-35 promotes macrophage survival and improves wound healing after myocardial infarction in mice, *Circ. Res.* 124 (9) (2019) 1323–1336.
- [41] K. Shirakawa, J. Endo, M. Kataoka, Y. Katsumata, N. Yoshida, T. Yamamoto, S. Isobe, H. Moriyama, S. Goto, H. Kitakata, T. Hiraide, K. Fukuda, M. Sano, IL (Interleukin)-10-STAT3-Galectin-3 Axis is essential for osteopontin-producing reparative macrophage polarization after myocardial infarction, *Circulation* 138 (18) (2018) 2021–2035.
- [42] Z. Dong, X. Zhao, W. Tai, W. Lei, Y. Wang, Z. Li, T. Zhang, IL-27 attenuates the TGF- $\beta$ 1-induced proliferation, differentiation and collagen synthesis in lung fibroblasts, *Life Sci.* 146 (2016) 24–33.
- [43] K.T. Weber, Y. Sun, E. Guarda, L.C. Katwa, A. Ratajska, J.P. Cleutjens, G. Zhou, Myocardial fibrosis in hypertensive heart disease: an overview of potential regulatory mechanisms, *Eur. Heart J.* 16 (Suppl C) (1995) 24–28.
- [44] R.A. Kastelein, C.A. Hunter, D.J. Cua, Discovery and biology of IL-23 and IL-27: related but functionally distinct regulators of inflammation, *Annu. Rev. Immunol.* 25 (2007) 221–242.
- [45] D.E. Dostal, R.A. Hunt, C.E. Kule, G.J. Bhat, V. Karoor, C.D. McWhinney, K.M. Baker, Molecular mechanisms of angiotensin II in modulating cardiac function: intracardiac effects and signal transduction pathways, *J. Mol. Cell. Cardiol.* 29 (11) (1997) 2893–2902.
- [46] P.A. Lalit, A.M. Rodriguez, K.M. Downs, T.J. Kamp, Generation of multipotent induced cardiac progenitor cells from mouse fibroblasts and potency testing in *ex vivo* mouse embryos, *Nat. Protoc.* 12 (5) (2017) 1029–1054.
- [47] G.W. Booz, J.N. Day, K.M. Baker, Interplay between the cardiac renin angiotensin system and JAK-STAT signaling: role in cardiac hypertrophy, ischemia/reperfusion dysfunction, and heart failure, *J. Mol. Cell. Cardiol.* 34 (11) (2002) 1443–1453.
- [48] E. Mascareno, M. El-Shafei, N. Maulik, M. Sato, Y. Guo, D.K. Das, M.A. Siddiqui, JAK/STAT signaling is associated with cardiac dysfunction during ischemia and reperfusion, *Circulation* 104 (3) (2001) 325–329.
- [49] P.K. Mehta, K.K. Griendling, Angiotensin II cell signaling: physiological and pathological effects in the cardiovascular system, *Am. J. Physiol. Cell Physiol.* 292 (1) (2007) C82–C97.
- [50] Q. Bao, B. Zhang, Y. Suo, C. Liu, Q. Yang, K. Zhang, M. Yuan, M. Yuan, Y. Zhang, G. Li, Intermittent hypoxia mediated by TSP1 dependent on STAT3 induces cardiac fibroblast activation and cardiac fibrosis, *Elife* 9 (2020).